Dynamical effects in proton-proton bremsstrahlung for non-coplanar geometries

Huisman, H.; Bacelar, J.C.S; van Goethem, M.J.; Harakeh, M.N.; Hoefman, M.; Kalantar-Nayestanaki, N.; Löhner, H.; Messchendorp, J.G.; Ostendorf, R.W.; Schadmand, S.

Published in:
Physics Letters B

DOI:
10.1016/s0370-2693(00)00130-1

Publication date:
2000

ELSEVIER

9 March 2000

PHYSICS LETTERS B

Physics Letters B 476 (2000) 9–14

Dynamical effects in proton–proton bremsstrahlung for non-coplanar geometries

H. Huisman [a], J.C.S. Bacelar [a], M.J. van Goethem [a], M.N. Harakeh [a], M. Hoefman [a], N. Kalantar-Nayestanaki [a,1], H. Löhner [a], J.G. Messchendorp [a,2], R.W. Ostendorf [a], S. Schadmand [a,2], O. Scholten [a], R.S. Simon [b], R.G.E. Timmermans [a], M. Volkerts [a], H.W. Wilschut [a]

[a] *Kernfysisch Versneller Instituut, Zernikelaan 25, 9747 AA Groningen, The Netherlands*
[b] *Gesellschaft für Schwerionenforschung, Planckstraße 1, 64291 Darmstadt, Germany*

Received 22 January 2000; accepted 28 January 2000
Editor: V. Metag

Abstract

The proton–proton bremsstrahlung process, including both coplanar and non-coplanar kinematics, has been measured with polarized protons of 190 MeV. High-precision cross sections and analyzing powers have been obtained. Cross sections as a function of non-coplanarity angle are presented and show large variations of dynamical origin. Non-coplanar analyzing powers have been measured for the first time and are compared to theoretical predictions.

PACS: 13.75.Cs; 25.10.+s; 25.20.Lj

Nucleon–nucleon bremsstrahlung, $N + N \rightarrow N + N + \gamma$, is the simplest process from which information can be obtained about the interacting two-nucleon system, beyond what is already known from elastic *NN* scattering and the deuteron [1–4]. According to the soft-photon theorem [5], the first two terms in an expansion of the bremsstrahlung amplitude in photon momentum are found from elastic scattering. Since the elastic nucleon–nucleon phase shifts are accurately known, a bremsstrahlung experiment aiming to probe new aspects of the *NN* interaction should measure hard-photon production at kinematics far away from the elastic limit. In non-relativistic elastic scattering, the opening angle between the scattered nucleons is always 90°. Therefore, measurements on nucleon–nucleon bremsstrahlung should preferably be performed at forward scattering angles with small opening angles.

In contrast with elastic scattering, the bremsstrahlung kinematics does not restrict the (initial and) final momenta to a plane. This is a general feature of reactions which have three particles in the final state where one can define a non-coplanarity angle which is a measure of how far out of plane the reaction products are. Measurements which particularly aim

[1] E-mail: nasser@kvi.nl
[2] Present address: Universität Gießen, Heinrich-Buff-Ring 16, 35392 Gießen, Germany.

0370-2693/00/$ - see front matter
PII: S0370-2693(00)00130-1

at effects as a function of non-coplanarity angle are scarce and performed at large proton scattering angles [6]. With the advent of detectors with large acceptances [7–10], measurements have been performed which cover a large part of the allowed non-coplanarity angles for reactions involving, for example, pion and photon production in nucleon–nucleon collisions. Due to the low reaction cross sections involved, the data have in the past been integrated over many variables including very often the non-coplanarity angle, in order to increase the statistical accuracy [11,12].

In this Letter, we report on the $pp\gamma$ cross sections and analyzing powers for non-coplanar geometries at 190 MeV beam energy. As we will show, there are sizable dynamical effects present as a function of this particular angle and if these effects are not taken into account properly when the data are being integrated over this angle, this can lead to wrong comparisons with theoretical calculations. In fact, it is argued that this variable is as important as any other variable in presenting differential cross sections. Finally, in experiments with a polarized beam, the non-coplanar geometry provides two other components of the analyzing power in addition to A_y which is obtained in coplanar geometry. We measured, for the first time, two of the three non-coplanar analyzing powers with high accuracy. The detection setup allowed to measure all three reaction products in coincidence. The total number of identified bremsstrahlung events is about 8 million for the whole experiment, resulting in the most precise measurement to date on this reaction.

The kinematics of proton–proton bremsstrahlung (which is similar to any reaction with a 3-body final state) was first described in detail by Drechsel and Maximon [13]. A brief discussion of the kinematics is given here, in order to define the different analyzing powers. The *z*-axis is defined by the incoming beam. In the case of coplanar scattering, where the momenta of all reaction products lie in one plane, the *x*-axis is defined orthogonal to the *z*-axis and in the scattering plane. The *y*-axis is defined such that it completes the right-handed set of orthogonal axes. In the case of non-coplanar scattering, the choice of the *x*- and *y*-axes is no longer unique. In our convention the scattering plane is defined by the incoming beam (*z*-axis) and the photon momentum. The *x*- and the *y*-axes are then defined as above with respect to this scattering plane. Furthermore, we define an external coordinate system with the *y*-direction in the direction of beam polarization. The angle ϕ_γ shown in Fig. 1 describes the rotation with respect to the external coordinates. The non-coplanarity angle is defined by $\Phi = |\pi/2 - |\phi_1 - \phi_2|/2|$, where ϕ_1 and ϕ_2 are the azimuthal angles of the two protons in the coordinate system just defined. Fig. 1 depicts the non-coplanarity angle for a typical $pp\gamma$ event.

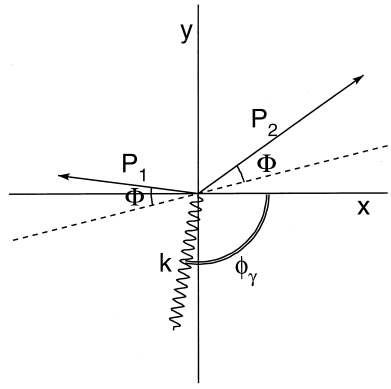

Fig. 1. A typical $pp\gamma$ event as projected on a plane perpendicular to the beam direction. Shown are the *external x* and *y*-axes, where the latter is defined by the direction of beam polarization. The beam comes out of the page.

A complicating feature of the differential cross section in the spherical coordinate system $(d\sigma/d\Omega_1 d\Omega_2 d\theta_\gamma)$ is that it diverges at the maximum of the non-coplanarity angle which depends on the polar angles of the outgoing particles. This divergence is due to the phase-space factor and has no dynamical origin. Several methods have been proposed to overcome this problem. For instance, a non-singular coordinate system can be chosen [6,14,15]. We have chosen to present the invariant Squared Matrix Element (SME), $|\mathcal{M}|^2$, [16,17]. If the phase-space factor is defined as J, the relation between the experimental cross section and SME is given by

$$\frac{d\sigma}{d\Omega_1 d\Omega_2 d\theta_\gamma}\Big|_{\text{exp}} = \frac{1}{\text{binsize}} \int_{\text{bin}} J|\mathcal{M}|^2 d\Omega_1 d\Omega_2 d\theta_\gamma \approx |\mathcal{M}|^2 \frac{1}{\text{binsize}} \int_{\text{bin}} J d\Omega_1 d\Omega_2 d\theta_\gamma . \quad (1)$$

Here, the plausible assumption is made that SME is constant over the bin. The expression for J is given in Ref. [13], see Eq. (3.9). The unit of J is $\mathrm{MeV}^2/(\mathrm{sr}^2\ \mathrm{rad})$. By dividing by $(\hbar c)^2$, SME obtains the unit $\mu\mathrm{b\ fm}^2$. In this unit, the magnitude of SME is in the order of 1.

If one defines σ^{pol} as the cross section for polarized particles and σ^u as the cross section for unpolarized particles, which is independent of ϕ_γ (but in principle dependent on Φ), then the most general form the cross section can take is

$$\begin{aligned}\frac{d\sigma^{\mathrm{pol}}}{d\Omega_1 d\Omega_2 d\theta_\gamma} &= \frac{d\sigma^u}{d\Omega_1 d\Omega_2 d\theta_\gamma}(1+\boldsymbol{P}\cdot\boldsymbol{A}) \\ &= \frac{d\sigma^u}{d\Omega_1 d\Omega_2 d\theta_\gamma}\left(1+pA_\gamma^\perp\cos\phi_\gamma+pA_\gamma\sin\phi_\gamma\right).\end{aligned} \tag{2}$$

Here, we introduce $A_\gamma^\perp$ and A_γ, which are equivalent to A_y and A_x, to denominate the analyzing powers. The reason for the different labels here is that the names A_y and A_x are more commonly associated with a different definition of the scattering plane [13]. In Eq. (2) the dependence on A_z is not shown, since it can only be measured with a polarization component in the direction of the beam, which was not present in our experiment. In coplanar kinematics, $A_\gamma = 0$ and $A_\gamma^\perp$ reduces to A_y.

For the measurement of the outgoing protons the Small-Angle Large-Acceptance Detector (SALAD) was used. This detector was specifically designed and built for these experiments. The design and operation of this detector is described in Ref. [10]. It has a large solid angle of 400 msr and allows to make cylindrically-symmetric measurements around the beam axis for most of the polar angular range. The covered polar angles range from 6° to 26°. The detector consists of two wire chambers [18] with a central hole for beam passage, behind which two segmented stacks of scintillators are mounted. The system is capable of handling high count rates and allows a hardware trigger rejection of protons stemming from elastic scattering [19]. This is achieved by choosing the thickness of the first scintillator stack such that elastically-scattered protons (which have a higher energy) punch through and reach the second stack. Also, a coincidence with the photon detection system is required.

For the measurement of the bremsstrahlung photons, we used the Two-Arm Photon Spectrometer, TAPS [20]. TAPS consists of approximately 400 BaF_2 crystals, which were used in two different geometries. In the first geometry, all crystals were mounted at backward angles in a large hexagon, surrounding the beam pipe. This results in a polar angular range of 125°–170° and a *complete* azimuthal coverage. This cylindrical symmetry makes it possible to determine the amplitudes of $\sin\phi_\gamma$ and $\cos\phi_\gamma$ in Eq. (2), which correspond to A_γ and $A_\gamma^\perp$, respectively. In order to investigate the angular distribution of the photons, a second experiment was performed where the cylindrical symmetry in photon detection was sacrificed. This second geometry, consists of six rectangular detector blocks, each containing 64 crystals. These blocks were positioned around the target on both sides of the beam pipe. In this geometry, the azimuthal range of photon detection at forward angles is centered around 0° and 180°. Therefore, at forward photon angles only $A_\gamma^\perp$ is obtained. At more backward angles the azimuthal coverage is larger, allowing a determination of A_γ with a somewhat larger error.

Only 2% of the collected events which satisfy the hardware trigger condition are good bremsstrahlung events, the rest being background that could not be eliminated by the trigger. In order to obtain a clean bremsstrahlung signal from the data, a cut is set on time-of-flight in TAPS to discriminate massive particles from photons. The reconstruction of events by exploiting the necessary set of five measured variables and the use of the other four measured variables in the overdetermined kinematics of the reaction results in a negligible background level [21].

For an accurate determination of the observables, one also needs to determine the luminosity and the degree of beam polarization. This is done by comparing the measured angular distribution of *pp* elastic scattering with two phase-shift analyses, from Nijmegen [1] and VPI [22]. A fit was made with only the luminosity and the beam polarization as a free parameter. The agreement with both phase-shift analyses is excellent. The typical value for the degree of

beam polarization is 0.65, with an accuracy of 0.01. For a discussion on detection efficiencies see Ref. [21]. The systematic error on the normalization of the cross-section data is 5%. The point-to-point systematic error is mainly due to errors in the determination of the wire-chamber efficiency and is 2%. The error in the analyzing powers is dominated by statistics.

Here, the data are presented as a function of the non-coplanarity angle. A sample of coplanar data has already been published in Ref. [21]. For a given θ_γ and asymmetric proton angles, one has two allowed kinematical solutions which are, in general, different in reaction dynamics. Due to energy and momentum conservation, the non-coplanarity angle, defined earlier, has a kinematic maximum. It can be shown that with increasing non-coplanarity angles, the two solutions converge to each other as one reaches the maximum allowed non-coplanarity. Having seen the large differences in SME for the two solutions in the coplanar reaction, it can be argued that SME must vary as a function of non-coplanarity.

In Fig. 2 the cross sections, SMEs and analyzing powers A_γ and $A_\gamma^\perp$ are shown as a function of the non-coplanarity angle. Both proton polar-scattering angles are fixed at 8°, while the photon polar-scattering angle is fixed at 145°. For this photon emission angle, it was possible to choose the combination of $\theta_1 = \theta_2 = 8°$ which is the smallest opening angle subtended by SALAD, resulting in the largest kinematically possible non-coplanarity angular range. The

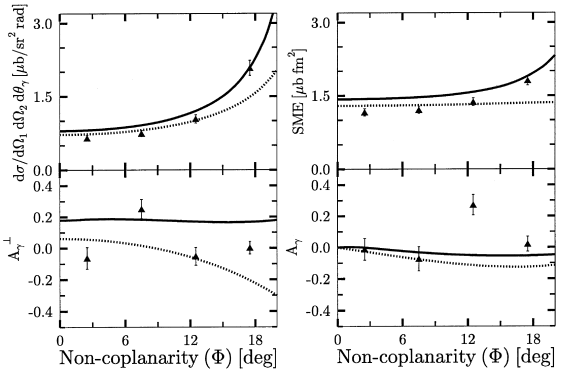

Fig. 2. Cross sections, SMEs and analyzing powers, A_γ and $A_\gamma^\perp$, as a function of the non-coplanarity angle. The proton polar angles have been fixed at 8°, while the photon polar angle is fixed at 145°. The solid and dotted curves are the results of the microscopic and SPA calculations, respectively. The maximum non-coplanarity angle for this kinematics is around 24°.

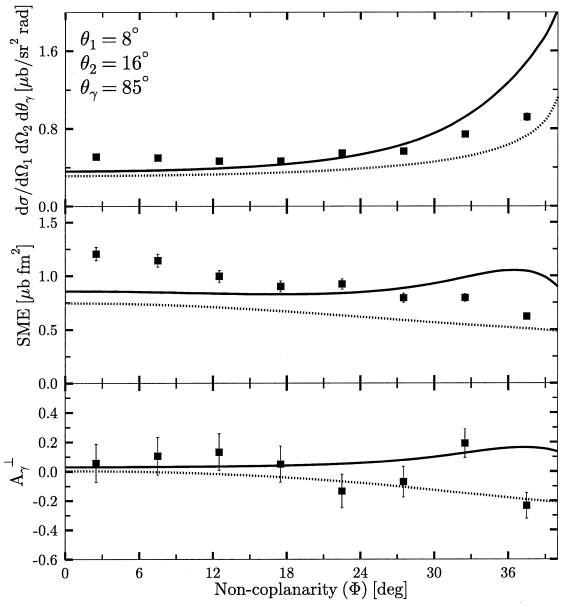

Fig. 3. Cross sections, SMEs and the analyzing power $A_\gamma^\perp$ as a function of the non-coplanarity angle. The proton polar angles have been fixed at 8° and 16°, while the photon polar angle is fixed at 85°. The meaning of the curves is the same as in Fig. 2. The maximum non-coplanarity angle for this kinematics is around 41.5°.

triangles shown in the figure are the average of the two measurements mentioned earlier, which are in excellent agreement. The bin size in proton polar angle is 2° and the bin size in photon polar angle is 10°. The non-coplanarity angle is varied from 0° to close to the kinematic maximum ($\approx 20°$). The bin size in non-coplanarity angle is 5°. The point at the non-coplanarity angle of 2.5° was considered to be coplanar in Ref. [21] (coplanarity angle runs from 0° to 90° in our convention.).

In Fig. 3 the cross sections, SMEs and the analyzing powers $A_\gamma^\perp$ are shown. The first proton polar angle is fixed at 8° while the second polar proton angle is fixed at 16°. The photon polar angle is fixed at 85°. The bin sizes are the same as above. For this photon emission angle, the proton angle combination of ($\theta_1 = 8°$, $\theta_2 = 16°$) is the smallest opening angle for which both proton energies are above the SALAD detection threshold, for all kinematically allowed non-coplanarity angles.

In both figures, the results of two calculations are also shown. The calculations shown by dotted lines

in all the plots are the predictions of the generalized Soft-Photon Amplitude (SPA) [23,24]. The solid curves in the plots represent the results of a calculation based on a microscopic model [25]. This model includes, apart from the single scattering, also the rescattering terms, magnetic meson-exchange currents, the virtual Δ-isobar and negative-energy states. The present data and also the data at coplanar geometry [21] lead to the conclusion that there are strong deficiencies in the models. Many of the detailed features observed in the present measurements would have been completely smeared out had the data been integrated over any of the differential variables showing how essential it is to have exclusive data.

An important feature of both kinematics presented here is that the SME varies smoothly but considerably (by up to a factor of 2) over the allowed range of non-coplanarity. This shows that part of the variations in the cross section as a function of this variable are of dynamical origin. When investigating the cross section directly, it is difficult to trace the dynamics, since it is masked by the trivial but wildly varying phase-space factors, especially near kinematical limits such as the maximum non-coplanarity angle. Taking a closer look at the kinematics of the reaction, one observes that spanning the non-coplanarity range, the relative energy between the two protons can go down to a few MeV at large non-coplanarity angles, implying that effects such as Coulomb distortions, which are neglected in many calculations, may play an important role here. Estimates have been made that these effects are small for the coplanar geometries presented in Ref. [21].

Examining the variations in SME as a function of various experimental variables reveals that there are sizable variations encountered independent of the variable. This points to the fact that the non-coplanarity angle is as important a variable as any other variable in presenting the differential cross sections in reactions with a 3-body final state.

In summary, a series of measurements on proton–proton bremsstrahlung have been performed at the beam energy of 190 MeV. The combined statistical and systematic error on the measurements is superior to any prior measurement of this process. Two different types of calculations are compared to the data, the first being a SPA, the other being a microscopic model. The comparison leads to the conclusion that in order to arrive at a complete picture of the reaction mechanism, one needs to have as exclusive data as possible. The presented SMEs for a large range of non-coplanarity angles unambiguously show that non-coplanarity effects of dynamical origin are important in this simple reaction with a 3-body final state. Furthermore, it was argued that the non-coplanarity angle is as important as any other variable in the presentation of the data. Two components of the analyzing power have been measured and presented at non-coplanar geometries for the first time. The variations observed in the analyzing powers are in general smaller than those observed in the SMEs. The present measurements yield a rather complete picture of the bremsstrahlung from the proton–proton system at a beam energy of 190 MeV and therefore provide a handle for future theoretical research on the nucleon–nucleon interaction.

Acknowledgements

The authors would like to acknowledge the support by the TAPS collaboration in bringing the Two-Arm Photon Spectrometer into operation at KVI. They also express their appreciation for the tireless efforts of the cyclotron and ion-source groups in delivering the high-quality beam used in these measurements. This work is part of the research program of the ''Stichting voor Fundamenteel Onderzoek der Materie'' (FOM) with financial support from the ''Nederlandse Organisatie voor Wetenschappelijk Onderzoek'' (NWO).

References

[1] M.C.M. Rentmeester, R.G.E. Timmermans, J.L. Friar, J.J. de Swart, Phys. Rev. Lett. 82 (1999) 4992.
[2] V.G.J. Stoks, R.A.M. Klomp, C.P.F. Terheggen, J.J. de Swart, Phys. Rev. C 49 (1994) 2950.
[3] R.B. Wiringa, V.G.J. Stoks, R. Schiavilla, Phys. Rev. C 51 (1995) 38.
[4] R. Machleidt, F. Sammarucca, Y. Song, Phys. Rev. C 53 (1996) R1483.
[5] F.E. Low, Phys. Rev. 110 (1958) 974.
[6] B. Gottschalk, W.J. Shlaer, K.H. Wang, Nucl. Phys. A 94 (1967) 491.
[7] H.O. Meyer et al., Phys. Rev. Lett. 81 (1998) 3096.
[8] WASA detector, TSL progress reports 1994-1995 and 1996-1997. See also the website http://www.tsl.uu.se/wasa.

[9] M. Dahmen et al., Nucl. Instrum. Methods Phys. Res., Sect. A 348 (1994) 97.
[10] N. Kalantar-Nayestanaki et al., Nucl. Instrum Methods Phys. Res., Sect. A, in press.
[11] B. von Przewoski et al., Phys. Rev. C 45 (1992) 2001.
[12] J. Zlomanczuk, A. Johansson, the WASA-PROMICE Collaboration, Nucl. Phys. A 631 (1998) 622c.
[13] D. Drechsel, L.C. Maximon, Ann. Phys. (NY) 49 (1968) 403.
[14] A. Katsogiannis, K. Amos, Phys. Rev. C 47 (1993) 1376.
[15] Yi Li, M.K. Liou, R. Timmermans, B.F. Gibson, Phys. Rev. C 58 (1998) R1880.
[16] O. Scholten, in: R.S. Simon (Ed.), Proc: TAPS workshop III, Bosen, September 1995, p. 67.
[17] H. Huisman, N. Kalantar-Nayestanaki, Phys. Rev. C, in press.
[18] M. Volkerts et al., Nucl. Instrum. Methods Phys. Res., Sect. A 428 (1999) 432.
[19] S. Schadmand et al., Nucl. Instrum. Methods Phys. Res., Sect. A 423 (1999) 174.
[20] H. Ströher, Nucl. Phys. News Int. 6 (1996) 7; A.R. Gabler et al., Nucl. Instrum. Methods Phys. Res., Sect. A 346 (1994) 168.
[21] H. Huisman et al., Phys. Rev. Lett. 83 (1999) 4017.
[22] R.A. Arndt et al., Phys. Rev. C 56 (1997) 3005.
[23] M.K. Liou, R.G.E. Timmermans, B.F. Gibson, Phys. Lett. B 345 (1995) 372; Phys. Rev. C 54 (1996) 1574.
[24] A.Yu. Korchin, O. Scholten, D. Van Neck, Nucl. Phys. A 602 (1996) 423.
[25] G.H. Martinus, O. Scholten, J.A. Tjon, Phys. Rev. C 56 (1997) 2945; Phys. Rev. C 58 (1998) 686.